

Poly(methyl methacrylate)-block-polyethylene-block-poly(methyl methacrylate) Triblock Copolymers as Compatibilizers for Polyethylene/Poly(methyl methacrylate) Blends

Yuewen Xu,[†] Christopher M. Thurber,[‡] Christopher W. Macosko,[‡] Timothy P. Lodge,^{*,†,‡} and Marc A. Hillmyer^{*,†}

[†]Department of Chemistry and [‡]Department of Chemical Engineering and Materials Science, University of Minnesota, Minneapolis, Minnesota 55455, United States

S Supporting Information

ABSTRACT: Poly(methyl methacrylate)-block-polyethylene-block-poly(methyl methacrylate) (PMMA–PE–PMMA) triblock copolymers were prepared by a combination of ring-opening metathesis polymerization (ROMP), hydrogenation, and reversible addition–fragmentation chain-transfer (RAFT) polymerization. The number-average molar masses of the PMMA end blocks were varied ($M_n = 1, 4, 12$, and 31 kg mol^{-1}), whereas that of the PE middle block was kept constant at $M_n = 13 \text{ kg mol}^{-1}$. The copolymers were evaluated as compatibilizers in PE/PMMA homopolymer blends containing PE in a 4:1 excess by weight. The compatibilized blends displayed significant improvements in elastic modulus, hardness, and scratch resistance as compared to uncompatibilized binary blends. The effects of the PMMA end-block molar mass and compatibilizer concentration on the blend morphology and mechanical properties were investigated. The triblock copolymer with the highest-molar-mass PMMA end blocks was most effective, presumably because of enhanced stress transfer between phases by virtue of a higher degree of entanglement of the end blocks with the PMMA dispersed phase.

INTRODUCTION

The commercial success of polyolefins is due in part to the low polarity, hydrophobicity, and resistance to harsh chemical environments of these macromolecular alkanes.^{1–4} However, because of their chemical structure, polyolefins are poorly compatible with more polar polymers.^{5–8} Compatibilizers are used to combat this deficiency and have been shown to be very effective in expanding the property profiles of polyolefin-based materials.^{9–21} Polyolefin block or graft copolymers are quite useful in improving the properties of polyolefin blends. For example, polyethylene-block-poly(methyl methacrylate) diblock copolymers (PE–PMMA) can effectively compatibilize polyolefin/poly(acrylate/methacrylate) blends.²² However, reports of such compounds are sparse, largely due to synthetic difficulties.^{23,24} In one example, a PE–PMMA diblock was produced by using $\text{SiMe}_2(\text{Ind})_2\text{ZrMe}_2$ and methylaluminoxane (MAO) cocatalyst through a sequential addition protocol.²⁵ Also, a hyperbranched PE macroinitiator was synthesized using a palladium diimine catalyst and a chloromethyl styrene chain-quenching agent. Copolymers of this hyperbranched PE and linear PMMA were then prepared by subsequent atom-transfer radical polymerization (ATRP).²⁶ Recently, we reported synthesis of the graft copolymer PE-graft-PMMA by ring-opening metathesis polymerization (ROMP) of cyclooctene (COE) with a functional bromo-COE, followed by ATRP “grafting from” of MMA. This graft copolymer was then applied as a compatibilizer in immiscible PE/PMMA blends.²⁷ Remarkably, the graft copolymers with the shortest PMMA grafts were most effective at improving the mechanical properties of the resulting ternary mixtures.

Stimulated by those results, we sought to explore the role of the compatibilizer molecular architecture in the efficacy of PE/PMMA compatibilization by investigating a series of poly(methyl methacrylate)-block-polyethylene-block-poly(methyl methacrylate) (PMMA–PE–PMMA) triblock copolymers by combining ROMP of COE in the presence of a chain-transfer agent and subsequent RAFT polymerization of methyl methacrylate. COE was first polymerized using Grubbs’ second-generation catalyst with a premade trithiocarbonate chain-transfer agent, as previously described by Mahanthappa et al.²⁸ Subsequent hydrogenation allowed the formation of a perfectly linear PE backbone bearing intact trithiocarbonate end groups. This PE macromolecular chain-transfer agent was then employed in the RAFT polymerization of MMA to give an ABA triblock copolymer. The effects of the PMMA end-block molar mass and compatibilizer concentration on the compatibilizer performance were assessed in terms of modulus, hardness, scratch resistance, and adhesion.

EXPERIMENTAL SECTION

Synthesis. Detailed synthetic procedures for the triblocks are provided in the Supporting Information.

Materials and Molecular Characterization. Linear low-density polyethylene (LLDPE, Exxon LL 3003) and high-density polyethylene (HDPE, 2S45SN) were obtained from ExxonMobil and The Dow Chemical Company, respectively.

Received: December 19, 2013

Revised: February 13, 2014

Accepted: February 26, 2014

Published: March 18, 2014



PMMA (Plexiglas MI-7) homopolymers were provided by Altuglas International. Grubbs' second-generation catalyst (**G2**) and 1,1'-azobis(cyclohexanecarbonitrile) were used as received from Sigma-Aldrich. Cyclooctene (*cis*-COE, 97%) was purchased from GFS Chemicals and purified by vacuum distillation. Methyl methacrylate was purified by being passed through a neutral alumina column and dried over molecular sieves. High-performance-liquid-chromatography (HPLC) grade chloroform was further purified by being passed through a basic alumina column and distilled over CaH_2 prior to polymerization. Other chemicals were used as received. Differential scanning calorimetry was performed on a TA Instruments Discovery Series DSC instrument. Polymer molar mass distributions were measured using a high-temperature size-exclusion-chromatography (SEC) system (PL-GPC 220, Agilent Systems) with 1,2,4-trichlorobenzene as the eluent (1.0 mL/min at 135 °C). The data were analyzed using a polystyrene standard calibration.

Preparation of PE/PMMA Blends. Polymer blends were prepared using a recirculating, conical twin screw extruder (DACA Instruments, 4 g capacity). Both stiff and rubbery PE matrixes (HDPE and LLDPE, respectively) were employed. Binary blends were prepared with 80 wt % HDPE (or LLDPE) and 20 wt % PMMA. For the compatibilized blend, the triblock copolymer was added at 1–5 wt % based on the total weight of the 80/20 blends. All components in each blend were premixed manually, introduced into the DACA instrument simultaneously, and melt mixed for 5 min at 200 rpm and 210 °C. The blend was then extruded and allowed to cool to room temperature.

Scanning Electron Microscopy (SEM). Polymer blends were subjected to cryomicrotoming at –140 °C and sputter coated with platinum (100 Å thickness) prior to SEM analysis. Images of samples were obtained using a JEOL 6700 scanning electron microscope at an accelerating voltage of 5 kV.

Tensile Testing. Tensile properties were investigated using a MINIMAT tensile tester (Rheometric Scientific) at an extension rate of 10 mm min^{−1}. All samples were prepared as dogbone shapes by compression molding (12 mm gauge length, 3 mm gauge width, 0.5 mm gauge thickness). Stress–strain curves were obtained and the elastic modulus (*E*, calculated from the slope of the initial linear portion of the stress–strain curve) and elongation at break (ϵ_b) were determined.

Adhesion Testing. Adhesion strength was assessed by 180° peel tests performed with a MINIMAT tensile tester.²⁹ PMMA and PE homopolymers were pressed into films by compression molding at 210 °C (~0.5 mm thickness). PMMA-*b*-PE-*b*-PMMA triblock copolymers were dissolved in benzene (0.03 g/13 mL) at 60 °C, and then PMMA films were dipped into this solution for a few seconds and air-dried. The triblock-copolymer-coated PMMA film and a premade PE film were pressed at 10 MPa to form a bilayer and laminated for 120 s at 180 °C^{6,30} prior to testing.

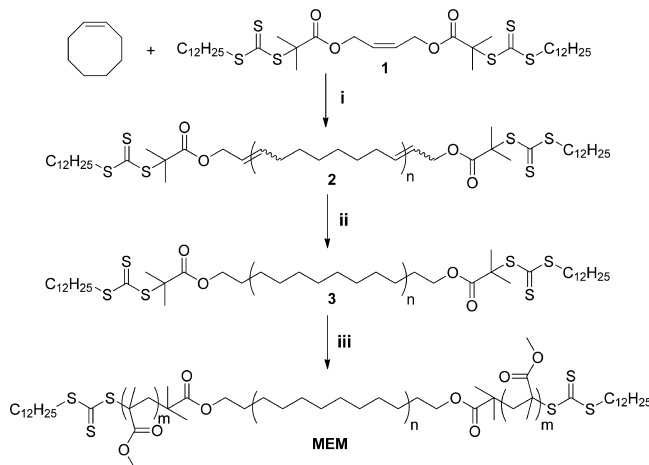
Nanoindentation. Nanoindentation tests were performed using a Nano Indenter (MTS System Co.). All polymer samples were pressed into films (~1 mm thickness) by compression molding and then mounted on an aluminum puck. For hardness tests, a Berkovich indenter was used at an approaching velocity of 10 ± 0.2 nm/s; hardness was calculated from P_{\max}/A of the load–displacement curve, where P_{\max} is the maximum loading force and A is the contact area between the tip and the polymer surface.³¹ A diamond indenter with a 90°

conical geometry was utilized for nanoscratch tests. A normal force was applied on the polymer surface, linearly increasing with lateral distance (from 0 to 40 mN). The scratch distance was recorded from 0 to 600 μm, and the force was first applied on the polymer surface at a distance of 100 μm.

RESULTS AND DISCUSSION

Preparation of PE Macromolecular CTA. The linear bifunctional PE macroinitiator **3** was prepared by ROMP of COE in the presence of the trithiocarbonate chain-transfer agent (CTA) **1**, followed by hydrogenation of the resulting telechelic polycyclooctene (Scheme 1). The molar mass of the

Scheme 1. Synthetic Route to PMMA-PE-PMMA^a



^aReagents and conditions: (i) **G2**, CHCl_3 , 40 °C; (ii) TsNNH_2 , tributylamine, *o*-xylene, 145 °C; (iii) MMA, toluene, 1,1'-azobis-(cyclohexanecarbonitrile), 100 °C.

polyCOE CTA (**2**) was controlled by the relative ratio between COE and **1** ($[\text{COE}]_0/[\text{1}]_0 = 90:1$). Low catalyst loadings ($[\text{COE}]_0/[\text{G2}]_0 \approx 4000:1$) were used to minimize the impact of the initial catalyst on the end functionality.³² Subsequent hydrogenation of the end-functionalized polycyclooctene utilizing *p*-toluenesulfonhydrazide (TsNNH_2) yielded the desired linear PE macromolecular CTA **3**.³³ Interestingly, the tosyl amine had no influence on the trithiocarbonate group, and the CTA was completely retained upon hydrogenation, as confirmed by ¹H NMR spectroscopy.

The ¹H NMR spectrum of macromolecular CTA **3** (Figure 1a) shows a broad singlet at 1.37 ppm corresponding to the PE backbone methylenes.³⁴ Two triplet signals at 4.01 and 3.83 ppm are associated with the methylene groups adjacent to ester and trithiocarbonate groups, respectively.²⁸ End-group analysis using the $-\text{CH}_3$ resonances at 0.92 ppm gave a number-average molar mass of 13 kg mol^{−1} (assuming exactly two trithiocarbonate end groups per chain). The molar mass dispersity of this macroinitiator was 1.7, which is not atypical for products from the ROMP of COE.³⁵

Preparation of PMMA-PE-PMMA. RAFT polymerization of methyl methacrylate was performed in toluene at elevated temperature (100 °C) to facilitate dissolution of **3**. 1,1'-Azobis(cyclohexanecarbonitrile) was used as a thermal initiator instead of 2,2'-azobisisobutyronitrile (AIBN), because of its longer half-life at elevated temperature.³⁶ Triblock copolymers with PMMA end-block molar masses of 1, 4, 12, and 31 kg mol^{−1} were prepared by controlling the polymer-

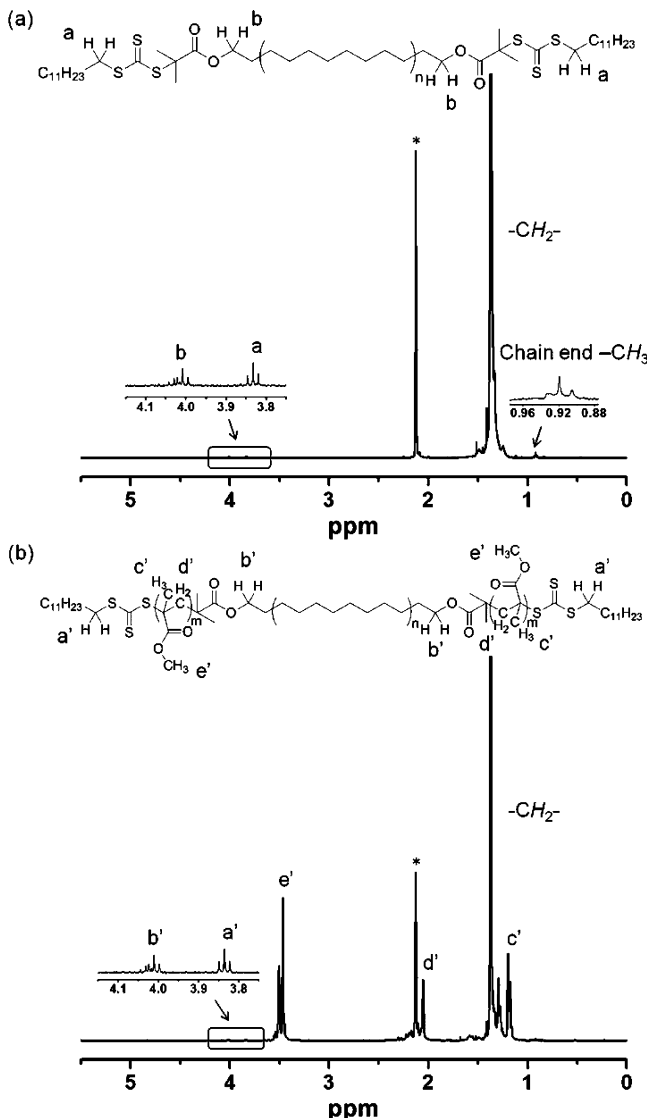


Figure 1. ^1H NMR spectra of (a) polyethylene macromolecular chain-transfer agent 3 and (b) PMMA-PE-PMMA (MEM) triblock copolymer. Toluene- d_8 at 100 °C; asterisk denotes residual protio solvent.

ization time (i.e., monomer conversion). The PMMA end-block molar masses were determined by relative integral ratios of corresponding blocks from ^1H NMR spectroscopy using the molar mass of the PE midblock. A range of molar masses were prepared, as high-molar-mass block copolymers could exhibit a low critical micelle concentration in blends and, thus, be less effective as interfacially active agents.³⁷ Although high-molar-mass block copolymers (>100 kg mol⁻¹) could affect coarsening and provide a better stabilization, they diffuse more slowly and are trapped in micelles at a lower concentration. Therefore, an intermediate range of molar masses was targeted to balance the ability to reach the interface and the compatibilizer effectiveness.³⁸ The molar mass of the PE middle block was well above its entanglement molar mass (ca. 1 kg mol⁻¹), whereas the relatively short PMMA blocks could facilitate diffusion to the PE/PMMA interface as implied in our work with PMMA graft polymers.²⁷

The molar masses and molar mass distributions of all of the polymers used in this study are listed in Table 1. The structure

Table 1. Molecular Characteristics of Homopolymers and Block Copolymers

	M_n (kg mol ⁻¹)	D^b	T_m^c (°C)	X_E^d (%)
	NMR ^a			
HDPE	25	2.8	131	71
LLDPE	50	3.9	123	43
PMMA ^e	45	1.8		
PE CTA 3	13	14	130	69
MEM[1–13–1]	15	16	129	55
MEM[4–13–4]	21	20	130	40
MEM[12–13–12]	37	34	129	17
MEM[31–13–31]	75	59	127	9

^aCalculated from NMR end-group analysis. ^bMeasured using a refractive-index (RI) detector on an SEC instrument with 1,2,4-trichlorobenzene at 135 °C. ^cDetermined from second heating, 10 °C/min. ^d X_E = degree of crystallinity, calculated based on PE content; ^e T_g (PMMA) = 104 °C. T_g of the PMMA component in MEM triblock could not be determined because of the broad melting transition of the PE block.

of the MEM triblock copolymer was confirmed by ^1H NMR spectroscopy (Figure 1b). The chemical shifts of the PE backbone signals were nearly identical to those of the PE macromolecular CTA 3. The chemical shifts at 3.45–3.50, 2.04, and 1.20 ppm correspond to the $-\text{OCH}_3$, $-\text{CH}_2-$, and $-\text{CH}_3-$ groups, respectively, on the PMMA block. Multiple signals at 3.45–3.5 ppm correspond to the enhanced syndiotacticity of PMMA.³⁹ The infrared spectrum also provided complementary evidence on the successful inclusion of PMMA blocks. Strong absorption bands at 1726 and 1146 cm⁻¹ are characteristic of stretching modes of $\nu(\text{C=O})$ and $\nu_a(\text{C—O—C})$ in the methyl methacrylate functionality.^{40,41} Precipitation of these copolymers in cold methanol gave monomodal triblocks with dispersities ranging from 1.8 to 2.0, as determined by SEC analysis (Figure S10, Supporting Information).

Blend Morphology. Although triblock copolymer compatibilizers have been studied,^{42–46} the role of molecular architecture in the efficacy of compatibilization has received less attention. A PE/PMMA blend with PMMA as the dispersed phase was targeted in an effort to improve the PE properties. PE/PMMA binary blends displayed irregular droplet shapes, larger droplet size dispersities, and larger number-average droplet sizes compared to those containing the PMMA-PE-PMMA triblocks.^{47,48} The dispersed PMMA phases showed decreasing domain sizes as the PMMA end-block molar masses in the PMMA-PE-PMMA compatibilized blends increased. This was true for both HDPE/PMMA and LLDPE/PMMA blends (Figures 2 and 3a). The average PMMA domain sizes in PE/PMMA blends containing MEM[31–13–31] decreased to 3.3 ± 0.9 and 2.2 ± 0.7 μm for HDPE/PMMA and LLDPE/PMMA blends, respectively (Figure 2e,j), as compared to the uncompatibilized binary blend.

The influence of the concentration of MEM[31–13–31] on droplet size was also investigated (Figure 3b). The droplet size was reduced by 50% with as low as 1 wt % MEM[31–13–31] in both HDPE/PMMA and LLDPE/PMMA blends. With the inclusion of more triblock copolymer, the particle size decreased slightly and appeared to level off; a low concentration of MEM[31–13–31] was sufficient to reduce interfacial tension in these blends.^{49,50} We then calculated the interfacial

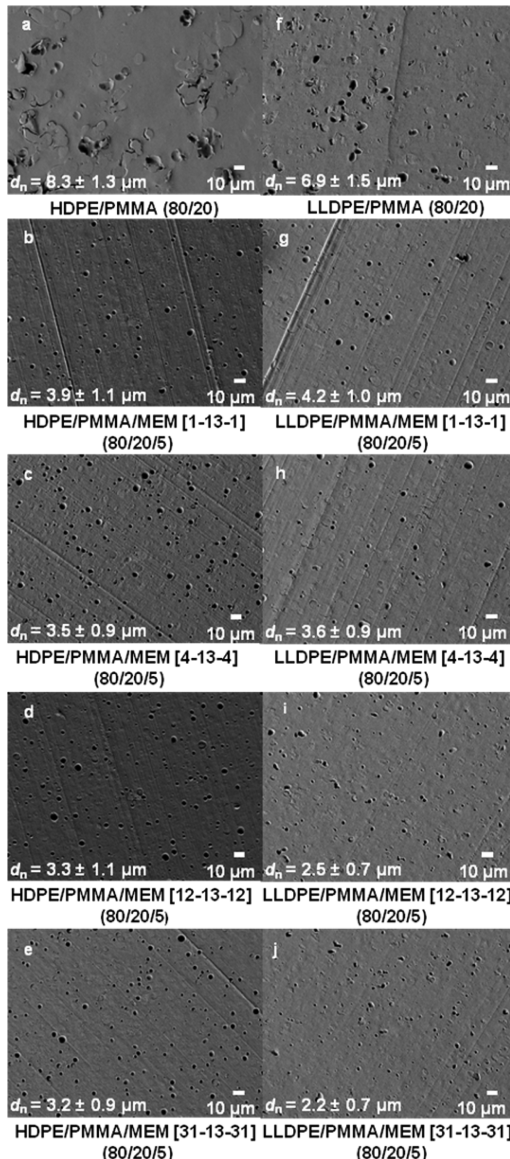


Figure 2. SEM images of different blends used. Scale bar represents 10 μm . About 200 particles were circled manually, and the number-average diameters (d_n) were determined using ImageJ software.

area occupied per triblock chain, assuming that all of the molecules resided at interface.^{51,52} In the HDPE/PMMA blends, the areal density of MEM[31–13–31] was 3.8, 1.5, and 0.8 nm^2/chain for 1, 2.5, and 5 wt %, respectively; in the LLDPE/PMMA blends, it was 5.8, 2.3, and 1.2 nm^2/chain for 1, 2.5, and 5 wt %, respectively.

Tensile and Hardness Evaluation. The mechanical properties of these polymer blends before and after compatibilization were examined to evaluate the efficacy of the compatibilizers.⁵³ Tensile tests were performed to determine the elastic modulus and elongation at break, whereas hardness values from nanoindentation provide useful information on the resistance of the polymer to a permanent shape change under force. High-density polyethylene (HDPE) is a stiff material with an elastic modulus of 550 MPa and an ultimate elongation of 320%, whereas linear low-density polyethylene (LLDPE) is a softer material with an elastic modulus of 110 MPa and an ultimate elongation of 1300%

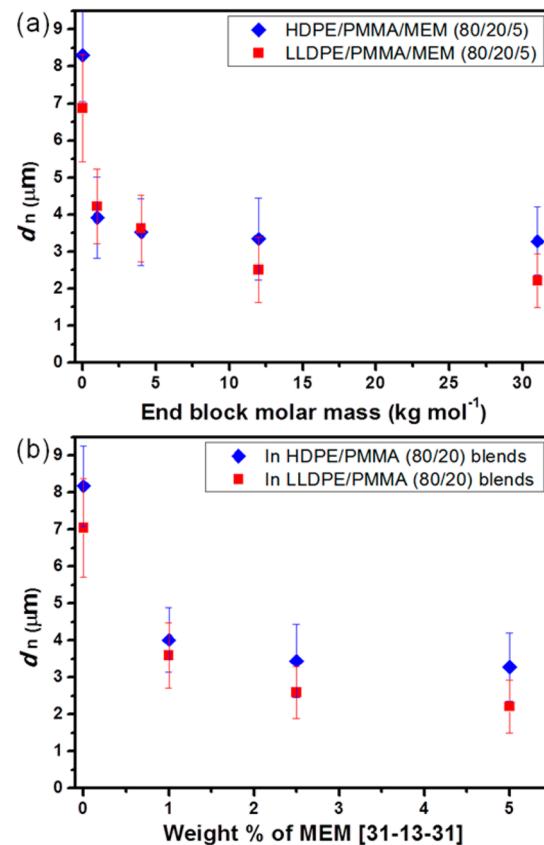


Figure 3. Droplet size for (a) PE/PMMA blends containing MEM triblock copolymers with different PMMA end-block molar masses (5 wt % MEM used for each blend) and (b) PE/PMMA (80/20) blends with MEM[31–13–31] at different mass concentrations of compatibilizer. Number-average particle diameter $d_n = \sum n_i d_i / \sum n_i$.

(Table 2). PMMA served as a hard phase in the blends because of its high elastic modulus of 2.1 GPa and hardness of 150 MPa.

The blends showed significant increases in elastic modulus and hardness when MEM triblock copolymers were introduced as compatibilization agents, as compared to the binary blends. As the end-block molar mass of the triblock increased, the elastic modulus and hardness of the blends increased. We attribute this behavior to the enhanced mechanical interlocking of PMMA chains at the interface and, thus, improved stress transfer from the hard phase to the polyethylene matrix (observed for both HDPE/PMMA and LLDPE/PMMA blends). Notably, the elastic modulus of the HDPE/PMMA blend with 5% MEM[31–13–31] achieved 1.0 GPa, although low elongation-at-break values were observed ($\epsilon_b \approx 5\%$, Table 2 and Figure 4a). The low elongation is likely due to the inability of the interface to debond or of the PMMA to cavitate, resulting in brittle failure.^{54,55} Upon application of the softer LLDPE, the elastic modulus of the compatibilized blend with the same triblock MEM[31–13–31] surpassed that of the corresponding binary blend by 80% (up to 270 MPa) while still retaining high elongation-at-break values (e.g., 630%).

Figure 4b shows the blend modulus as a function of compatibilizer concentration. At as low as 1% compatibilizer inclusion, the elastic modulus of the compatibilized blend with MEM[31–13–31] surpassed that of the binary blend by 15% and 48% for the HDPE/PMMA and LLDPE/PMMA systems, respectively. Such high efficiency suggests that the MEM triblock was able to bridge the matrix and dispersed phase and

Table 2. Mechanical Properties of Homopolymers and Polymer Blends

	modulus (MPa)	hardness (MPa)	elongation at break (%)	final penetration depth ^a (μm)
PMMA	2100 \pm 80	150 \pm 10	49 \pm 9	4.4 \pm 0.5
HDPE	550 \pm 40	62 \pm 5	320 \pm 50	11 \pm 0.8
LLDPE	110 \pm 9	17 \pm 2	1300 \pm 60	20 \pm 0.8
HDPE/PMMA (80/20)	680 \pm 40	64 \pm 5	6.4 \pm 1.0	10 \pm 0.9
HDPE/PMMA/PE CTA 3 (80/20/5)	630 \pm 50	64 \pm 4	5.3 \pm 0.9	10 \pm 0.8
HDPE/PMMA/MEM[1–13–1] (80/20/5)	860 \pm 40	72 \pm 3	5.4 \pm 0.9	7.3 \pm 0.4
HDPE/PMMA/MEM[4–13–4] (80/20/5)	880 \pm 30	73 \pm 3	5.3 \pm 0.9	7.1 \pm 0.6
HDPE/PMMA/MEM[12–13–12] (80/20/5)	910 \pm 40	75 \pm 3	5.1 \pm 0.5	6.7 \pm 0.5
HDPE/PMMA/MEM[31–13–31] (80/20/5)	1000 \pm 30	81 \pm 3	4.1 \pm 0.5	6.4 \pm 0.4
LLDPE/PMMA (80/20)	150 \pm 30	19 \pm 4	800 \pm 90	37 \pm 3.0
LLDPE/PMMA/PE CTA 3 (80/20/5)	140 \pm 30	19 \pm 3	720 \pm 60	31 \pm 2.8
LLDPE/PMMA/MEM[1–13–1] (80/20/5)	190 \pm 20	21 \pm 2	720 \pm 50	15 \pm 1.2
LLDPE/PMMA/MEM[4–13–4] (80/20/5)	240 \pm 20	23 \pm 2	700 \pm 40	13 \pm 0.9
LLDPE/PMMA/MEM[12–13–12] (80/20/5)	250 \pm 20	24 \pm 2	650 \pm 40	12 \pm 0.7
LLDPE/PMMA/MEM[31–13–31] (80/20/5)	270 \pm 20	27 \pm 2	630 \pm 40	11 \pm 0.7

^aThe penetration depth at the scratch distance of 600 μm in the nanoindentation test.

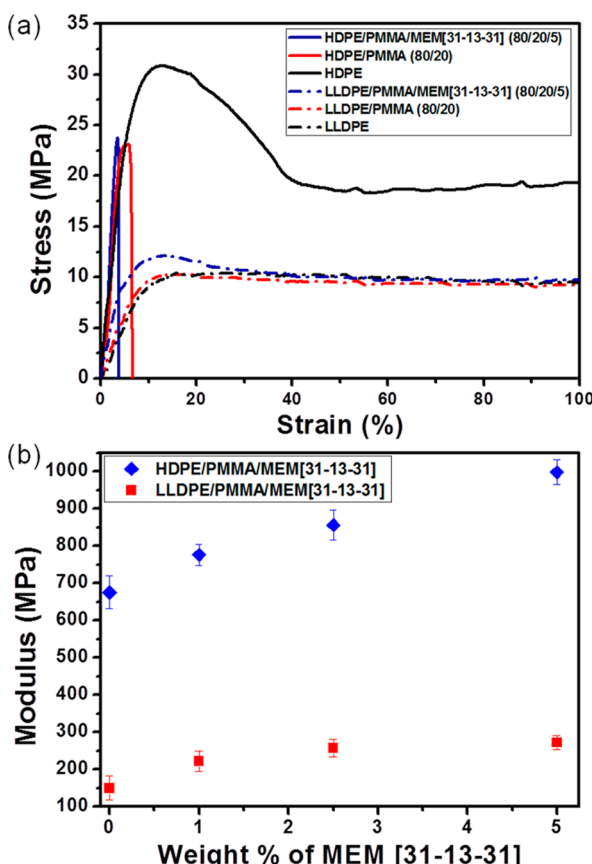


Figure 4. (a) Representative stress-strain curves for PE homopolymers and uncompatibilized and compatibilized blends at low strain. (b) Elastic modulus for HDPE/PMMA and LLDPE/PMMA blends with MEM[31–13–31] as the compatibilizer at different mass ratios.

transfer stress across the interface effectively even at low concentrations.

Adhesion. SEM images of cross sections of fracture surfaces from tensile tests provide a straightforward sense of the interfacial adhesion and stress transfer across the interface. In the absence of triblock copolymers, very distinct surfaces around PMMA particles were observed in both HDPE/PMMA

and LLDPE/PMMA blends, suggesting little or no adhesion between the two polymers (Figure 5a,c). However, with MEM[31–13–31], significant roughness at the particle surface suggested efficient stress transfer between the PMMA hard phase and the PE matrix (Figure 5b,d).

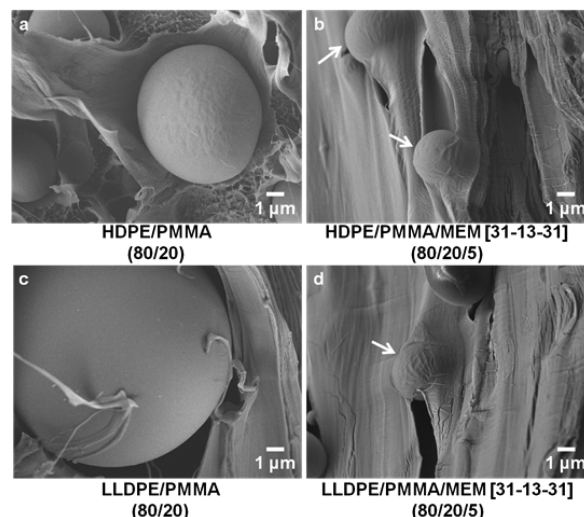


Figure 5. SEM images of fracture surfaces after tensile testing.

Peel tests were used to obtain direct quantitative measurements of the influence of the triblock copolymer on the interfacial adhesion between PMMA and the two PE homopolymers.^{56,57} Virtually no adhesion was observed between PMMA and the two PE homopolymers, as they readily delaminated. In contrast, the triblock-copolymer-coated system gave appreciable adhesion (Figure 6). Increased adhesion strength was observed with increasing end-block molar mass of PMMA, which was likely due to the enhanced interlocking of the entangled PMMA chains. The HDPE/MEM triblock-coated PMMA system generally exhibited a slightly higher adhesion strength than the LLDPE system, an effect plausibly due to a higher miscibility between the perfectly linear PE midblock of the MEM triblock and the HDPE, as well as the

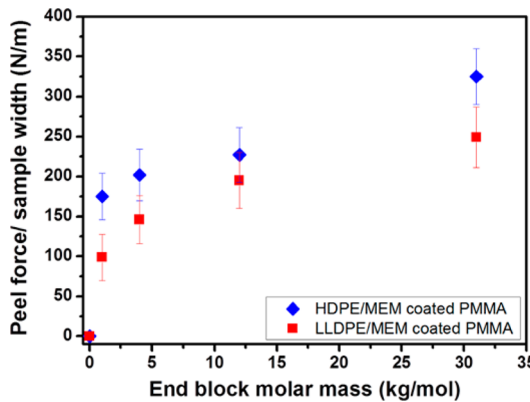


Figure 6. Peel force/sample width for adhesion between PE and MEM triblock-coated PMMA films at different MEM end-block molar masses.

enhanced ability of the midblock and matrix phase to cocrystallize.⁵⁴

Scratch Resistance. In the nanoscratch test, a conical indenter tip was placed on the polymer surface and moved laterally for 100 μm. Then, a normal force was applied, linearly increasing with distance, from 0 to 40 mN over 500 μm. The scratch resistance thus is reflected in the penetration depth into the polymer surface at the final scratch length.^{58,59} The scratch resistance of PMMA homopolymer is high, because of its high rigidity and lower tendency to undergo plastic-flow-induced scratch damage (Figure 7 and Table 2). Both PE homopol-

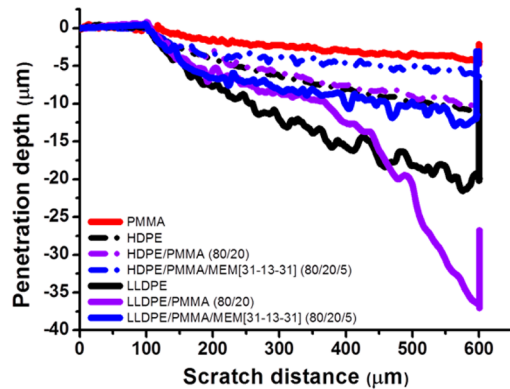


Figure 7. Penetration depth vs scratch distance profiles for PE and PMMA homopolymers and PE/PMMA blends.

ymers were found to have poor scratch resistance, although the HDPE was more resistant to scratching than the LLDPE because of its inherent stiffness. The compatibilized blends with triblock copolymers displayed significant improvements in reducing indenter penetration depths under applied force, as compared to the corresponding PE homopolymers and binary blends, indicating an enhanced scratch resistance. It is notable that the HDPE/PMMA blend with 5% MEM[31–13–31] revealed a scratch resistance that was comparable to that of the PMMA homopolymer, considering that PE was applied as the matrix material.

The elastic modulus plays an important role in scratch behavior, especially in the indentation stage.⁶⁰ A certain degree of rigidity of the polymer is necessary to resist plastic flow.⁶¹ This correlates well with our PE/PMMA systems and related systems,⁶² as compatibilized blends had a relatively high

modulus and were more resistant to scratching. Other material surface characteristics, such as yield stress, friction coefficient, and scratch hardness, have also been found to be responsible for the scratch behavior of polymeric materials, although the detailed mechanisms including the formation of cracks and debonding in multiphase thermoplastic polyolefins (TPO) are still under investigation.⁶³

Comparison of Graft and Triblock Copolymers as Compatibilizers. Recently, we demonstrated that PE-g-PMMA copolymers are effective compatibilizers in LLDPE/PMMA (70/30) blends. The graft copolymer with the shortest graft (31 wt % PMMA; six MMA repeat units per graft, denoted as PE-g-PMMA_6) was found to be the most effective compatibilizer, and we attributed this result to the kinetic limitations in partitioning of the graft copolymer to interface with higher-molar-mass grafts.²⁷ Indeed, in new experiments, we demonstrated that the blending time in PE-g-PMMA_6-compatibilized blends had minimal impact on PMMA droplet size and modulus (comparing 5–40 min of melt blending time). In contrast, LLDPE/PMMA/PE-g-PMMA_24, with 24 repeat units per graft (70/30/5), clearly displayed a reduction in PMMA droplet size from 4.6 to 2.7 μm as the blend time increased from 5 to 40 min (Table 3). In the case of the

Table 3. Comparison of Graft and Triblock Copolymers at Different Melt Blending Times

	blend time (min)	droplet size (μm)	elastic modulus (MPa)
PE-g-PMMA_6 ^a	5	2.3 ± 0.5	255 ± 15
PE-g-PMMA_6	40	2.3 ± 0.6	257 ± 12
PE-g-PMMA_24	5	4.6 ± 0.9	240 ± 15
PE-g-PMMA_24	40	2.7 ± 0.7	253 ± 14
MEM[1–13–1] ^b	5	4.2 ± 0.7	190 ± 20
MEM[1–13–1]	40	4.0 ± 0.5	190 ± 15
MEM[31–13–31]	5	2.2 ± 0.5	270 ± 20
MEM[31–13–31]	40	2.4 ± 0.6	268 ± 17

^aPE-g-PMMA stands for polyethylene-graft-poly(methyl methacrylate). The graft copolymer contains a PE backbone with a number-average molar mass of $M_n = 30 \text{ kg mol}^{-1}$ and 21 side chains on average. All graft copolymers here refer to LLDPE/PMMA/PE-g-PMMA (70/30/5) blends; ^bAll triblock copolymers here refer to LLDPE/PMMA/MEM (80/20/5) blends.

PMMA–PE–PMMA triblock-compatibilized blends, there was no significant influence of blending time on the morphology, regardless of the PMMA end-block molar mass, with both HDPE and LLDPE (Figure S14, Supporting Information). Furthermore, both MEM[1–13–1] and MEM[31–13–31] gave equivalent droplet sizes and elastic modulus values in LLDPE/PMMA (80/20) blends containing 5 wt % compatibilizer when the melt blending time was increased from 5 to 40 min (Table 3).

These results suggest that the kinetic partitioning of PE–PMMA copolymers to the PE/PMMA interface was much more profound when the graft copolymer with longer side chains was used, likely because the inherent multiple grafting sites on the PE backbone prevented the rapid diffusion of long side chains at short blending times. In the case of triblock copolymer, minimal kinetic effects during melt blending were observed, as there was no significant morphological change between triblock PE/PMMA systems blended for 5 min and those blended for 40 min.

CONCLUSIONS

We prepared PMMA-*b*-PE-*b*-PMMA triblock copolymers for the first time by combining ROMP of *cis*-cyclooctene in the presence of a trithiocarbonate CTA, hydrogenation, and RAFT polymerization of methyl methacrylate. Triblock copolymers with different PMMA end-block molar masses were prepared to study the influence of the PMMA molar mass on the efficiency of the compatibilizer in PE/PMMA(80/20) homopolymer blends. Both stiff HPDE and soft LLDPE matrix materials were applied in this study. The blends containing these triblock copolymers showed significant improvements in blend morphology, elastic modulus, hardness, and scratch resistance as compared to the noncompatibilized versions. As the molar mass of the PMMA end blocks in the MEM triblock increased, the material properties improved, likely because of the enhanced entanglement density and increased interfacial width at the PE/PMMA interface. The HDPE/PMMA compatibilized blends gave maximum modulus, hardness, and scratch resistance, whereas the compatibilized blends with LLDPE as the matrix had enhanced mechanical properties with respect to those of the binary blends while remaining ductile. The effective loading concentration of compatibilizers in PE/PMMA blends was also studied, and it was found that as little as 1% compatibilizer gave significant improvements in properties. Adhesion tests suggest that these triblock copolymers are effective adhesion promoters, providing a pathway to connect incompatible PE and methacrylate-based polymers.

ASSOCIATED CONTENT

Supporting Information

Detailed synthesis of MEM triblock copolymers; ^1H NMR, ^{13}C NMR, and FTIR spectra of all polymers; representative stress-strain curves. This material is available free of charge via the Internet at <http://pubs.acs.org>.

AUTHOR INFORMATION

Corresponding Authors

*E-mail: lodge@umn.edu (T.P.L.).

*E-mail: hillmyer@umn.edu (M.A.H.).

Notes

The authors declare no competing financial interest.

ACKNOWLEDGMENTS

This work was funded by The Dow Chemical Company. We thank Craig Silvis from Dow for helpful input and guidance during these studies. Part of this work was carried out in the College of Science and Engineering Polymer Characterization Facility, University of Minnesota, which has received capital equipment funding from the NSF through the UMN MRSEC program, Award DMR-0819885.

REFERENCES

- (1) Peacock, A. J. *Handbook of Polyethylene: Structure, Properties, and Applications*; Marcel Dekker: New York, 2000.
- (2) Atiqullah, M.; Tinkl, M.; Pfaendner, R.; Akhtar, M. N.; Hussain, I. Synthesis of functional polyolefins using metallocenes: A comprehensive review. *Polym. Rev.* **2010**, *50*, 178.
- (3) Piringer, O. G.; Baner, A. L. *Plastic Packaging: Interactions with Food and Pharmaceuticals*, 2nd ed.; Wiley-VCH: Weinheim, Germany, 2008.
- (4) Chung, T. C. Synthesis of functional polyolefin copolymers with graft and block structures. *Prog. Polym. Sci.* **2002**, *27*, 39.
- (5) Kobori, Y.; Akiba, I.; Akiyama, S. Compatibilizing effects of poly(ethylene-*b*-methyl methacrylate) on blends of polyethylene and poly(4-vinylphenol). *Polymer* **2000**, *41*, 5971.
- (6) Song, J.; Ewoldt, R. H.; Hu, W.; Silvis, H. C.; Macosko, C. W. Flow accelerates adhesion between functional polyethylene and polyurethane. *AIChE J.* **2011**, *57*, 3496.
- (7) Schellekens, M.; Klumperman, B. Synthesis of Polyolefin Block and Graft Copolymers. *J. Macromol. Sci., Polym. Rev.* **2000**, *40*, 167.
- (8) Chung, T. C. *Functionalization of Polyolefins*; Academic Press: New York, 2002.
- (9) Li, Y.; Yakovleva, V.; Chen, H.; Hiltner, A.; Baer, E. Comparison of olefin copolymers as compatibilizers for polypropylene and high-density polyethylene. *J. Appl. Polym. Sci.* **2009**, *113*, 1945.
- (10) Ho, C.-H.; Wang, C.-H.; Lin, C.-I.; Lee, Y.-D. Synthesis and characterization of TPO-PLA copolymer and its behavior as compatibilizer for PLA/TPO blends. *Polymer* **2008**, *49*, 3902.
- (11) Mishra, J. K.; Hwang, K.-J.; Ha, C.-S. Preparation, mechanical and rheological properties of a thermoplastic polyolefin (TPO)/organoclay nanocomposite with reference to the effect of maleic anhydride modified polypropylene as a compatibilizer. *Polymer* **2005**, *46*, 1995.
- (12) Scaffaro, R.; La Mantia, F. P.; Canfora, L.; Polacco, G.; Filippi, S.; Magagnini, P. Reactive compatibilization of PA6/LDPE blends with an ethylene-acrylic acid copolymer and a low molar mass bis-oxazoline. *Polymer* **2003**, *44*, 6951.
- (13) Lai, S.-M.; Yeh, F.-C.; Wang, Y.; Chan, H.-C.; Shen, H.-F. Comparative study of maleated polyolefins as compatibilizers for polyethylene/wood flour composites. *J. Appl. Polym. Sci.* **2003**, *87*, 487.
- (14) Retolaza, A.; Eguiazabal, J. I.; Nazabal, J. A lithium ionomer of poly(ethylene-*co*-methacrylic acid) copolymer as compatibilizer for blends of poly(ethylene terephthalate) and high density polyethylene. *Polym. Eng. Sci.* **2002**, *42*, 2072.
- (15) Stutz, H.; Heckmann, W.; Potschke, P.; Wallheinke, K. Structural effects of compatibilizer localization and effectivity in thermoplastic polyurethane-polyolefin blends. *Appl. Polym. Sci.* **2002**, *83*, 2901.
- (16) Akpalu, Y. A.; Karim, A.; Satija, S. K.; Balsara, N. P. Suppression of Lateral Phase Separation in Thin Polyolefin Blend Films. *Macromolecules* **2001**, *34*, 1720.
- (17) Papadopoulou, C. P.; Kalfoglou, N. K. Comparison of compatibilizer effectiveness for PET/PP blends: Their mechanical, thermal and morphology characterization. *Polymer* **2000**, *41*, 2543.
- (18) Benderly, D.; Siegmann, A.; Narkis, M. Polymer encapsulation of glass filler in ternary PP/PA-6/glass blends. *Polym. Compos.* **1996**, *17*, 86.
- (19) Kim, B. Y.; Park, S. Y.; Park, S. J. Morphological, thermal and rheological properties of blends: Polyethylene/nylon-6, polyethylene/nylon-6/(maleic anhydride-g-polyethylene) and (maleic anhydride-g-polyethylene)/nylon-6. *Eur. Polym. J.* **1991**, *27*, 349.
- (20) Kim, D. H.; Fasulo, P. D.; Rodgers, W. R.; Paul, D. R. Effect of the ratio of maleated polypropylene to organoclay on the structure and properties of TPO-based nanocomposites. Part II: Thermal expansion behavior. *Polymer* **2008**, *49*, 2492.
- (21) Ratnayake, U. N.; Haworth, B. Polypropylene-clay nanocomposites: Influence of low molecular weight polar additives on intercalation and exfoliation behavior. *Polym. Eng. Sci.* **2006**, *46*, 1008.
- (22) Harrats, C.; Jerome, R. Block balance in hydrogenated polybutadiene-*b*-polymethylmethacrylate diblock copolymer for efficient interfacial activity in low-density polyethylene/polymethylmethacrylate blend: Phase morphology development. *J. Polym. Sci. B: Polym. Phys.* **2005**, *43*, 837.
- (23) Kawahara, N.; Kojoh, S.; Matsuo, S.; Kaneko, H.; Matsugi, T.; Saito, J.; Kashiwa, N. Synthetic method of polyethylene-poly(methylmethacrylate) (PE-PMMA) polymer hybrid via reversible addition-fragmentation chain transfer (RAFT) polymerization with functionalized polyethylene. *Polym. Bull.* **2006**, *57*, 805.
- (24) Inoue, Y.; Matsugi, T.; Kashiwa, N.; Matyjaszewski, K. Graft copolymers from linear polyethylene via atom transfer radical polymerization. *Macromolecules* **2004**, *37*, 3651.

- (25) Atiqullah, M.; Hossain, M. M.; Kamal, M. S.; Al-Harthi, M. A.; Khan, M. J.; Hossaen, A.; Hussain, I. Crystallization kinetics of PE-*b*-isotactic PMMA diblock copolymer synthesized using $\text{SiMe}_2(\text{Ind})_2\text{ZrMe}_2$ and MAO cocatalyst. *AIChe J.* **2013**, *59*, 200.
- (26) Wang, W.-J.; Liu, P.; Li, B.-G.; Zhu, S. One-step synthesis of hyperbranched polyethylene macroinitiator and its block copolymers with methyl methacrylate or styrene via ATRP. *J. Polym. Sci. A: Polym. Chem.* **2010**, *48*, 3024.
- (27) Xu, Y.; Thurber, C. M.; Lodge, T. P.; Hillmyer, M. A. Synthesis and Remarkable Efficacy of Model Polyethylene-*graft*-poly(methyl methacrylate) Copolymers as Compatibilizers in Polyethylene/poly(methyl methacrylate) Blends. *Macromolecules* **2012**, *45*, 9604.
- (28) Mahanthappa, M. K.; Bates, F. S.; Hillmyer, M. A. Synthesis of ABA Triblock Copolymers by a Tandem ROMP—RAFT Strategy. *Macromolecules* **2005**, *38*, 7890.
- (29) Sato, E.; Tamura, H.; Matsumoto, A. Cohesive Force Change Induced by Polyperoxide Degradation for Application to Dismantlable Adhesion. *ACS Appl. Mater. Interfaces* **2010**, *2*, 2594.
- (30) Kobayashi, S.; Song, J.; Silvis, H. C.; Macosko, C. W.; Hillmyer, M. A. Amino-Functionalized Polyethylene for Enhancing the Adhesion between Polyolefins and Polyurethanes. *Ind. Eng. Chem. Res.* **2011**, *50*, 3274.
- (31) Oliver, W.; Pharr, G. Measurement of hardness and elastic modulus by instrumented indentation: Advances in understanding and refinements to methodology. *J. Mater. Res.* **2011**, *19*, 3.
- (32) Pitet, L. M.; Chamberlain, B. M.; Hauser, A. W.; Hillmyer, M. A. Synthesis of Linear, H-Shaped, and Arachnearn Block Polymers by Tandem Ring-Opening Polymerizations. *Macromolecules* **2010**, *43*, 8018.
- (33) Hahn, S. F. An improved method for the diimide hydrogenation of butadiene and isoprene containing polymers. *J. Polym. Sci. A: Polym. Chem.* **1992**, *30*, 397.
- (34) Kaneyoshi, H.; Inoue, Y.; Matyjaszewski, K. Synthesis of Block and Graft Copolymers with Linear Polyethylene Segments by Combination of Degenerative Transfer Coordination Polymerization and Atom Transfer Radical Polymerization. *Macromolecules* **2005**, *38*, 5425.
- (35) Bielawski, C. W.; Grubbs, R. H. Living ring-opening metathesis polymerization. *Prog. Polym. Sci.* **2007**, *32*, 1.
- (36) Mukumoto, K.; Wang, Y.; Matyjaszewski, K. Iron-Based ICAR ATRP of Styrene with ppm Amounts of $\text{Fe}^{\text{III}}\text{Br}_3$ and 1,1'-Azobis-(cyclohexanecarbonitrile). *ACS Macro Lett.* **2012**, *1*, 599.
- (37) Macosko, C. W.; Guegan, P.; Khandpur, A. K.; Nakayama, A.; Marechal, P.; Inoue, T. Compatibilizers for Melt Blending: Premade Block Copolymers. *Macromolecules* **1996**, *29*, 5590.
- (38) Galloway, J. A.; Jeon, H. K.; Bell, J. R.; Macosko, C. W. Block copolymer compatibilization of cocontinuous polymer blends. *Polymer* **2005**, *46*, 183.
- (39) White, A. J.; Filisko, F. E. Tacticity determination of poly(methyl methacrylate) (PMMA) by high-resolution NMR. *J. Polym. Sci.: Polym. Lett. Ed.* **1982**, *20*, 525.
- (40) Willis, H. A.; Zichy, V. J. I.; Hendra, P. J. Low frequency dielectric behavior of polyamides. *Polymer* **1968**, *10*, 737.
- (41) Emmons, E. D.; Kraus, R. G.; Duvvuri, S. S.; Thompson, J. S.; Covington, A. M. High-pressure infrared absorption spectroscopy of poly(methyl methacrylate). *J. Polym. Sci. B: Polym. Phys.* **2007**, *45*, 358.
- (42) Wu, D.; Zhang, Y.; Yuan, L.; Zhang, M.; Zhou, W. Viscoelastic interfacial properties of compatibilized poly(ϵ -caprolactone)/polylactide blend. *J. Polym. Sci. B: Polym. Phys.* **2010**, *48*, 756.
- (43) Vranjes, N.; Lednický, F.; Kotek, J.; Baldrian, J.; Rek, V.; Fortelny, I.; Horák, Z. Compatibilization efficiency of styrene-butadiene block copolymers as a function of their block number. *J. Appl. Polym. Sci.* **2008**, *108*, 466.
- (44) Souza, A. M. C.; Demarquette, N. R. Influence of coalescence and interfacial tension on the morphology of PP/HDPE compatibilized blends. *Polymer* **2002**, *43*, 3959.
- (45) Macaubas, P. H. P.; Demarquette, N. R. Morphologies and interfacial tensions of immiscible polypropylene/polystyrene blends modified with triblock copolymers. *Polymer* **2001**, *42*, 2543.
- (46) Radonjic, G.; Musil, V.; Smit, I. Compatibilization of polypropylene/polystyrene blends with poly(styrene-*b*-butadiene-*b*-styrene) block copolymer. *J. Appl. Polym. Sci.* **1998**, *69*, 2625.
- (47) Lohse, D. J.; Datta, S.; Kresge, E. N. Graft Copolymer Compatibilizers for Blends of Polypropylene and Ethylene-Propylene Copolymers. *Macromolecules* **1991**, *24*, 561.
- (48) Khatua, B. B.; Lee, D. J.; Kim, H. Y.; Kim, J. K. Effect of Organoclay Platelets on Morphology of Nylon-6 and Poly(ethylene-*ran*-propylene) Rubber Blends. *Macromolecules* **2004**, *37*, 2454.
- (49) Tang, T.; Huang, B. Interfacial behaviour of compatibilizers in polymer blends. *Polymer* **1994**, *35*, 281.
- (50) Thomas, S.; Prud'homme, R. E. Compatibilizing effect of block copolymers in heterogeneous polystyrene/poly(methyl methacrylate) blends. *Polymer* **1992**, *33*, 4260.
- (51) Guegan, P.; Macosko, C. W.; Ishizone, T.; Hirao, A.; Nakahama, S. Kinetics of Chain Coupling at Melt Interfaces. *Macromolecules* **1994**, *27*, 4993.
- (52) Matos, M.; Favis, B. D.; Lomellini, P. Interfacial modification of polymer blends—The emulsification curve: 1. Influence of molecular weight and chemical composition of the interfacial modifier. *Polymer* **1995**, *36*, 3899.
- (53) Mandal, P. K.; Siddhanta, S. K.; Chakraborty, D. Engineering properties of compatibilized polypropylene/liquid crystalline polymer blends. *J. Appl. Polym. Sci.* **2012**, *124*, 5279.
- (54) Anderson, K. S.; Hillmyer, M. A. The influence of block copolymer microstructure on the toughness of compatibilized polylactide/polyethylene blends. *Polymer* **2004**, *45*, 8809.
- (55) Bartczak, Z.; Argon, A. S.; Cohen, R. E.; Weinberg, M. Toughness mechanism in semi-crystalline polymer blends: II. High-density polyethylene toughened with calcium carbonate filler particles. *Polymer* **1999**, *40*, 2347.
- (56) Shenton, M. J.; Lovell-Hoare, M. C.; Stevens, G. C. Adhesion enhancement of polymer surfaces by atmospheric plasma treatment. *J. Phys. D: Appl. Phys.* **2001**, *34*, 2754.
- (57) Kumar, K. D.; Tsou, A. H.; Bhowmick, A. K. Interplay between bulk viscoelasticity and surface energy in autohesive tack of rubber-tackifier blends. *J. Polym. Sci. B: Polym. Phys.* **2010**, *48*, 972.
- (58) Pelletier, H.; Mendibide, C.; Riche, A. Mechanical characterization of polymeric films using depth-sensing instrument: Correlation between viscoelastic-plastic properties and scratch resistance. *Prog. Org. Coat.* **2008**, *62*, 162.
- (59) Brostow, W.; Kovacevic, V.; Vrsaljko, D.; Whitworth, J. Tribology of polymers and polymer-based composites. *J. Mater. Educ.* **2010**, *32*, 273.
- (60) Xiang, C.; Sue, H. J.; Chu, J.; Coleman, B. Scratch behavior and property relationship in polymers. *J. Polym. Sci. B: Polym. Phys.* **2001**, *39*, 47.
- (61) Manias, E.; Touney, A.; Wu, L.; Strawhecker, K.; Lu, B.; Chung, T. C. Polypropylene/ Montmorillonite Nanocomposites. Review of the Synthetic Routes and Materials Properties. *Chem. Mater.* **2001**, *13*, 3516.
- (62) Song, J.; Thurber, C. M.; Kobayashi, S.; Baker, A.; Macosko, C. W.; Silvis, H. C. Blends of polyolefin/PMMA for improved scratch resistance, adhesion and compatibility. *Polymer* **2012**, *53*, 3636.
- (63) Krupicka, A.; Johansson, M.; Hult, A. Use and interpretation of scratch tests on ductile polymer coatings. *Prog. Org. Coat.* **2003**, *46*, 32.